

Plasmon excitations in homogeneous neutron star matter.

M. Baldo and C. Ducoin

Dipartimento di Fisica, Università di Catania

and

INFN, Sezione di Catania

Via S. Sofia 64, I-95123, Catania, Italy

ABSTRACT

We study the possible collective plasma modes which can affect neutron-star thermodynamics and different elementary processes in the baryonic density range between nuclear saturation (ρ_0) and $3\rho_0$. In this region, the expected constituents of neutron-star matter are mainly neutrons, protons, electrons and muons ($npe\mu$ matter), under the constraint of beta equilibrium. The elementary plasma excitations of the $pe\mu$ three-fluid medium are studied in the RPA framework. We emphasize the relevance of the Coulomb interaction among the three species, in particular the interplay of the electron and muon screening in suppressing the possible proton plasma mode, which is converted into a sound-like mode. The Coulomb interaction alone is able to produce a variety of excitation branches and the full spectral function shows a rich structure at different energy. The genuine plasmon mode is pushed at high energy and it contains mainly an electron component with a substantial muon component, which increases with density. The plasmon is undamped for not too large momentum and is expected to be hardly affected by the nuclear interaction. All the other branches, which fall below the plasmon, are damped or over-damped.

PACS : 21.65.+f , 24.10.Cn , 26.60.+c , 03.75.Ss

I. INTRODUCTION

The evolution of neutron stars is in general determined by the microscopic processes that can occur in their interior and in their crust. In particular, the cooling process by neutrino emission is strongly affected by the detailed structure of the matter and the excitations it can sustain. Mean free path and emissivity of neutrinos are directly related to the correlations present in the neutron star matter, which in the standard models is composed of neutrons, protons, electron and muons [1]. The effect of collective excitations on neutrino emissivity have been extensively studied in the literature, often with controversial results [2–8]. The proton plasmon excitations seem to play a relevant role in quenching the contribution of the pair-breaking mode to neutrino emissivity [5] by charged current, since it obscures the possible effect of the Goldstone mode, which should be present in a superfluid due to gauge invariance. However at low momentum the electron and muon screening is quite effective and we will show that indeed the proton plasmon does not exist, and therefore its role in neutrino emissivity is quite delicate and must be examined with care. For the same reasons, at low momenta the proton oscillations are accompanied necessarily by electron and muon oscillations, and this can be of great relevance on the total neutrino emission [7]. The real plasmon mode in neutron star matter is at higher energy and we will show that it is mainly an electron excitation, with very small contribution of the proton motion but a non-negligible muon component.

All that can be best studied considering the proton, electron and muon spectral functions, that can be used also to determine the damping of each mode. We will present extensive results on the spectral functions of the electron-muon-proton plasma under neutron star physical conditions. Full spectrum and width of the excitations will be presented in detail.

Since neutron and proton are coupled by nuclear forces, it is not clear to what extent the presence of the plasmon mode can affect the whole set of collective excitations or the excitation spectrum at a qualitative level, even for non-superfluid matter. Some considerations and preliminary results will be presented on this point, which will stress that the genuine plasma excitations are in general approximately decoupled from the rest of the spectrum, but in particular cases

they can be strongly damped.

II. THE ELECTRON-MUON-PROTON PLASMA

We consider protons, muons and electrons, in neutron star matter conditions, interacting by Coulomb coupling, disregarding the nuclear interaction of protons with neutrons. This idealized case, which of course does not correspond to actual physical conditions, will permit to clarify two points, also relevant for the general physical situation. On one hand it will make more transparent the role of electron and muon screening on the proton dynamics, on the other hand it will give clear indications on the strengths of the electrons, muons and protons motion at the different excitation energies. The role of nuclear forces will be briefly discussed at the end of the Section.

As already mentioned in the Introduction, we are considering normal nuclear matter, leaving the case of superfluid matter to a future work. The range of total baryon density ρ_b will be fixed between the saturation density $\rho_0 = 0.16 \text{ fm}^{-3}$ and $3\rho_0$, where indeed neutron star matter is expected to be homogeneous and not affected by possible "exotic" components like hyperons. Of course the proton fraction $Y_p = \rho_p/\rho_b$ has to be fixed in order to choose the proton density, which is actually the only relevant parameter for the system under study. In order to specify Y_p according to neutron-star structure, it is determined by beta equilibrium, which depends on the nuclear matter EOS. This will be taken from the microscopic calculations of Ref. [9, 10], based on the many-body theory within the Bethe-Brueckner-Goldstone (BBG) scheme. For simplicity we will work at zero temperature, but the results can be easily extended to finite temperature. Electroneutrality imposes $\rho_p = \rho_e + \rho_\mu$, and the proportion between electrons and muons is fixed by chemical equilibrium. The resulting proton and muon fractions as a function of baryon density are reported in Fig. 1. On this figure, the microscopic calculations are compared with results from three modern Skyrme forces: SLy230a [11], NRAPR [12] and LNS [13], in order to give the order of magnitude of the dependence on the EOS. The particle fractions used for the three baryonic densities under study are listed in Tab. I.

For a one component plasma, i.e. a charged Fermi gas on a rigid uniform

background (jelly model), the Random Phase Approximation (RPA) has been studied in detail, both in the non-relativistic [14] and relativistic [15] cases. The excitation spectrum, i.e. the line in the energy-momentum plain where the real part of the polarization function has poles, is known to have a "thumb like" shape. This is illustrated in Fig. 2 (full line), where the case of a proton gas at a density $\rho = \rho_0$ is considered.

For future convenience, we report here the RPA equations for the polarization propagator $\Pi(k, \omega)$, which is a function of the momentum q and energy ω :

$$\Pi(q, \omega) = \Pi_0(q, \omega) + v_c(q)\Pi_0(q, \omega)\Pi(q, \omega). \quad (1)$$

Here $v_c(q) = 4\pi e^2/q^2$ is the proton-proton Coulomb interaction and $\Pi_0(q, \omega)$ is the free polarization propagator:

$$\Pi_0(k, \omega) = \int \frac{d^3k}{(2\pi)^3} \int \frac{d\omega'}{2\pi i} G_0(|\mathbf{k} + \mathbf{q}|, \omega + \omega') G_0(\mathbf{k}, \omega') \quad (2)$$

and $G_0(k, \omega)$ is the free single particle Green' s function

$$G_0(k, \omega) = \frac{\theta(k - k_F)}{E - E_k + i\eta} + \frac{\theta(k_F - k)}{E - E_k - i\eta}, \quad (3)$$

where E_k is the single particle energy, k_F the Fermi momentum and $\theta(x)$ the Heaviside step function, which equals 1 for $x > 0$ and is zero otherwise. The excitation spectrum is thus determined by the equation $\text{Re}(1 - v_c(k)\Pi_0(k, \omega)) = 0$. The explicit expression for the free polarization in the non-relativistic limit can be found in textbooks and is usually referred to as the Lindhard function. The upper branch appearing in Fig. 2 is called the plasmon excitation, which is characterized by a finite energy at vanishing momentum and has a simple classical interpretation [16]. The lower branch is actually strongly damped and does not correspond to a real excitation which is able to propagate. This point will be further elaborated in the sequel. From the Figure it is clear that in any case there is a maximum value of the momentum above which the spectrum stops and no excitation is possible. This is mainly a quantal effect, which is not present in the semi-classical approximation of RPA, which is nothing else than the Vlasov approximation. This is illustrated in the same Fig. 2, where the RPA and the Vlasov approximation (dashed lines) spectra are compared. Apart from the momentum cutoff, one can see that the spectra are quite similar. The results for

the relativistic case are analogous [15], except that the "thumb" becomes thinner and thinner as the Fermi momentum becomes more and more relativistic [17]. In the ultra-relativistic case the two branches become extremely close near the cutoff, and the difference between RPA and Vlasov spectrum appears smaller and smaller, apart again for the presence of the momentum cutoff. In the following, all the calculations will be performed in the Vlasov approximation for the three fluids, protons, electrons and muons.

Having summarized the well established results for the excitation spectrum with the pure Coulomb interaction within the jelly model, let us consider the system of protons, electrons and muons, treating the three components on equal footing. The RPA equations for this case are simply a three by three system, where the coupling is again provided by the Coulomb interaction between protons, muons and electrons:

$$\Pi^{ik}(q, \omega) = \Pi_0^{ii}(q, \omega) \left(\delta_{ik} + \sum_{j=e, \mu, p} v_c^{ij}(q) \Pi^{jk}(q, \omega) \right) . \quad (4)$$

The polarization propagator Π^{ik} is now a three by three matrix. In Eq. (4) the index i, j, k stands for electrons (e), muons (μ) and protons (p). These equations describe the motion of a three-component fluid. It has to be stressed that no exchange is included, i.e. only density-density correlations are considered. Since both electrons and muons are expected to be faster than protons, they are able to follow their motion and are more effective in screening the proton-proton interactions. The total spectrum is now formed by several branches, but only one is expected to have the characteristic property of a finite excitation energy at vanishing momentum, and this will be identified with the plasmon mode of the proton-muon-electron coupled system. The original proton plasmon mode becomes now a sound-like mode, since, due to the electron and muon screening, the effective proton-proton interaction becomes of finite range (screened Coulomb interaction). This is a well known phenomenon also in classical plasma [16]. The screening can be easily seen in the present case by solving Eqs. (4) for the proton-proton polarization propagator. After a short algebra one finds:

$$\left(1 - \Pi_0^{pp} \frac{v_c}{1 - (\Pi_0^{ee} + \Pi_0^{\mu\mu}) v_c} \right) \Pi^{pp} = \Pi_0^{pp} . \quad (5)$$

Since the unperturbed electron and muon plasmon modes are substantially higher than the corresponding proton one, in the small q limit one can expand the free

electron polarization propagator at zero frequency and one gets

$$\left(1 - \Pi_0^{pp} \frac{4\pi e^2}{q^2 + q_c^2}\right) \Pi^{pp} = \Pi_0^{pp}, \quad (6)$$

which is an RPA equation with a screened Coulomb interaction and therefore of finite range. For $q < q_c$ the collective mode can be only a sound mode with a typical linear dependence on momentum. The inverse $\lambda = 1/q_c$ is the screening length. One finds that $q_c^2 = 3[(\omega_p^e/v_F^e)^2 + (\omega_p^\mu/v_F^\mu)^2]$, where ω_p^e and ω_p^μ are the electron and muon gas plasmon frequencies, respectively, and v_F^e, v_F^μ the corresponding Fermi velocities. In neutron star matter conditions $q_c \ll k_F^p$ and the screening length is much larger than the average distance between protons. Therefore, at increasing momenta the proton excitation should merge in the proton plasmon mode with no screening. Besides that, the static limit we have performed in Eq. (6) is only approximately valid, especially at the higher density, where the proton plasma frequency is a substantial fraction of the electron plasma frequency, and it is more appropriate to solve explicitly Eq. (4). The actual calculations confirm these expectations, as illustrated in Fig. 3 for three proton densities corresponding to total baryon densities $\rho_0, 2\rho_0$ and $3\rho_0$. The reported branches are obtained by searching for the energies for which the determinant Δ of the real part of the three by three matrix in Eq. (4) vanishes at a given momentum. In the present particular case it has a simple expression:

$$\Delta = 1 - v_c(\Pi_0^{ee} + \Pi_0^{\mu\mu} + \Pi_0^{pp}) \quad (7)$$

One observes that all branches go to zero at vanishing momentum, except the upper one. The latter is the plasmon mode of the three components system, while the "thumb like" shape of the original proton branch in the uncoupled system can be identified with the lowest "loop" (color on line). Additional branches appear in between these two. For $\rho = \rho_0$ one additional branch approaches closely the plasmon one at increasing momentum. It can be considered as the original "sound like" electron mode, according to the above discussion for the proton gas in the jelly model. It turns out, as we will show below, that it is still mainly an electron excitation even in the coupled case. The last additional excitation, which looks also a "sound like" mode is reminiscent of a pure muon excitation, which however is now mixed with a small electron component. This coupling become

stronger at increasing density and the two branches merge in a single one with a typical "bending back", see panels for $\rho = 2\rho_0$ and $\rho = 3\rho_0$, which actually marks the smooth transition from almost a pure electron excitation to a mixed electron-muon excitation.

To support and illustrate this type of analysis we have reported in the same figure the branches (dashed lines) one obtains when one considers only protons and electrons. In this case, we keep the original proton density and substitute the electron-muon liquid by a pure electron liquid with $\rho_e = \rho_p$. From the figure one can trace the evolution of the branches when introducing the muon component. It has to be noticed that all branches, except the plasmon one, are actually damped. The polarization propagators Π_0 which appear in Eqs. (4) are indeed in general complex. The best way to estimate the damping rate of each branch is to calculate the spectral function $-\text{Im}(\Pi^i(q, \omega))$, which, in the present case, has a proton ($i = p$), an electron ($i = e$) and a muon ($i = \mu$) component. This quantity is also the basic one for calculating the rate of many physical processes. At a given momentum q , as a function of ω this quantity is expected to display peaks corresponding to the different branches, whose width gives a measure of their damping rate, i.e. each excitation mode is actually a resonance if the width is not too large. The plasmon, up to a certain momentum, has no width, and the strength function presents a delta function singularity at the plasmon frequency. The electron, muon and proton strength functions are reported in Fig. 4 at twice the saturation density and at selected values of the momentum q . For guidance, a dashed vertical line is reported at the position of each branch. To put in evidence the plasmon branch we have reported just a sharp bar at the position of its energy. One can see that that peaks are present at the energy corresponding to the branches of Fig. 3, even if some slight shifts occur. Such shifts are expected, since the presence of an imaginary part has also the effect to produce some displacements.

The relatively narrow peak at lower energy corresponds to the original proton plasmon in the uncoupled system. As discussed above, this branch in the coupled system is a sound-like mode due to electron and muon screening. For this branch the proton component is larger, but electrons and muons follow the proton oscillation, which allows a quite effective screening. However, as the momentum

increases the screening becomes less effective, in agreement with the discussion above. Besides that, the coupling with electrons and muons produces a substantial damping of this branch. At higher energy a small broad peak is obtained, which involves a substantial fraction of both muons and electrons, but not protons. This branch is a coupled oscillations of electrons and muons, which behave approximately as a single fluid. It is characteristic of the coupling between electrons and muons, and would not be present in a system with only protons and electrons. In any case, as one can see, the strength associated with this structure is quite low. It has to be noticed that it is present also at $q = 10$ MeV, where in principle no branch is present at this energy. The fact that this structure does not correspond to the vanishing of the real part of the RPA determinant is an indication that the corresponding oscillation is over-damped, and indeed it is quite broad at this momentum.

The very broad structure which appears just below the sharp plasmon peak is only due to the electrons, and it corresponds to the over-damped sound-like branch which is present in a single fluid, below the plasmon, as discussed for the proton case in relation with Fig. 2. Its strength is increasing at increasing momentum.

To illustrate and support these considerations and interpretations of the results, we compare in Fig. 5 at different densities and for $q = 10$ MeV the strength functions of the proton-muon-electron system with the ones of the two-component proton-electron system, where the electron density equals the electron-muon density of the three-component system. One can see that the electrons and muons move together in screening the proton plasmon, with a total strength not so far from the electron strength in the two-component system. As anticipated above, the broad electron-muon structure is not present in the two-component system, while the broad electron structure below the plasmon peak is mainly unaffected. However, at the lowest density one notices a muon peak just above the proton sound-like mode and a very weak involvement of the muons in the screening of the proton motion. The muon peak corresponds to the branch at "intermediate energy" in Fig. 3. This means that at this density the muons are not able to follow the proton motion and produce an independent mode, which however has not a plasmon-like character since its energy is mainly linear in momentum.

Let us analyze in more detail the plasmon mode, which is the highest in energy and appears in the spectral function as a delta-function singularity. In fact at the plasmon energy all the free propagators Π_0^{ii} are real. Solving the RPA equations, one gets:

$$\Pi^{ii} = \frac{\Pi_0^{ii}[1 - (\Pi_0^{jj} + \Pi_0^{kk})v_c]}{\Delta + i\eta}, \quad (8)$$

where $i \neq j \neq k$ and η is the usual infinitesimal quantity demanded by the general structure of the response function. The plasmon contribution to the spectral function is then:

$$-\text{Im}(\Pi^{ii}) = v_c(\Pi_0^{ii})^2\delta(\omega - \omega_p)/|\Delta(\omega_p)'| \quad (9)$$

where ω_p is the plasmon energy, solution of the equation $\Delta(\omega) = 0$. The ratios of the different strengths are then given by

$$\frac{\text{Im}(\Pi^{ii})}{\text{Im}(\Pi^{jj})} = \frac{(\Pi_0^{ii})^2}{(\Pi_0^{jj})^2}, \quad (10)$$

where the expression of Eq. (7) for the determinant has been used. The plasmon pole corresponds also to the zero eigenvalue of the RPA matrix which in Eq. (4) defines the response function $\Pi(\omega)$, i.e.

$$\sum_{j=e,\mu,p} (\delta_{ij} - \Pi_0^{ii}(\omega_p)v_c^{ij}(q)) \delta\rho_j = 0, \quad (11)$$

where the eigenvector $\delta\rho = (\delta\rho_e, \delta\rho_\mu, \delta\rho_p)$ describes the electron, muon and proton density fluctuations of the modes. One easily finds

$$\frac{\delta\rho_i}{\delta\rho_j} = z_i z_j \frac{\Pi_0^{ii}}{\Pi_0^{jj}}, \quad (12)$$

where $z_i = \pm 1$ is the charge sign of the i -component. This result is in agreement with Eq. (10), since the spectral function gives the *square* of the density fluctuation.

In Fig. 6 are reported some ratios of the density fluctuations, according to Eq. (12), which describes the plasmon mode at different momenta. The main characteristic to be noticed is the dominance of the electron component, with the muons becoming of some relevance only at the higher densities. The proton component is marginal, since protons are unable to follow the rapid motion of the negatively charged components. The momentum dependence is quite weak.

In the analysis we have carried out, the nuclear interaction and the presence of neutrons have been completely neglected. However, the plasmon mode is at relatively large frequency, while the nuclear sound (or zero-sound) mode starts linearly with momentum. The coupling between the plasmon and the other modes is expected to be quite weak, and the properties of the plasmon excitation are likely to be essentially unaffected. Furthermore, the plasmon mode is known not to be influenced by the possible presence of a superfluid phase [18].

The nuclear interaction can affect the lower energy modes, whose strength will be then redistributed. In particular the sound-like mode involving the protons will be coupled with neutron modes, since it falls in the low frequency part of the spectrum, due to the screening effect discussed above. This shows the relevance of the Coulomb interaction for the overall structure of the spectrum. A complete analysis of the excitation strength distribution, including both Coulomb and nuclear interaction, will be given elsewhere.

III. CONCLUSION AND PROSPECTS.

We have analyzed, within the RPA scheme, the plasmon excitations which can occur in the homogeneous matter present in the outer core of Neutron Stars. The proton, electron and muon components have been considered. Since both electron and muon Fermi velocity are larger than the proton one, the Coulomb proton-proton interaction is effectively screened and no genuine proton plasmon can exist, but instead a sound-like mode is present. The analysis of the spectral functions shows that the high frequency plasmon mode is mainly an electron excitation, with possibly a substantial muon component at higher density. Except for the genuine plasmon mode, all other excitation modes are damped, and in some case over-damped. The inclusion of the nuclear interaction and of the neutron component will be reported elsewhere.

[1] S.L. Shapiro and S.A. Teukolsky, *Black Holes, White Dwarfs and Neutron Stars* (Jhon Wiley and Sons, New York, 1983).

[2] D. G. Yakovlev, A. D. Kaminker and K. P. Levenfish, *A&A* 343 (1999) 650

- [3] S.Reddy, M. Prakash, J. Lattimer and J. Pons, Phys. Rev. C 59, 2888 (1999).
- [4] J. Kundu and S. Reddy, Phys. Rev. C 70, 055803 (2004).
- [5] L.B. Leinson and A. Perez, Phys. Lett. B 638, 114 (2006).
- [6] A. Sedrakian, H. Müther and P. Schuck, Phys. Rev. C 76, 055805 (2007).
- [7] L.B. Leinson, Phys. Rev. C 78, 015502 (2008)
- [8] E. E. Kolomeitsev and D. N. Voskresensky, arXiv:0802.1404 [astro-ph].
- [9] M. Baldo, I. Bombaci and G.F. Burgio, Astronomy and Astrophysics 328 (1997) 274.
- [10] X.R. Zhou, G.F. Burgio, U. Lombardo, H.-J. Schulze and W. Zuo, Phys. Rev. C 69 (2004) 018801.
- [11] E. Chabanat, P. Bonche, P. Haensel, J. Meyer and R. Schaeffer, Nucl. Phys. **A627**, 710 (1997);
- [12] A.W. Steiner, M. Prakash, J.M. Lattimer and P.J. Ellis, Phys. Rep. **411** 325 (2005).
- [13] L. G. Cao, U. Lombardo, C. W. Shen and N. Van Giai, Phys. Rev. C **73**, 014313 (2006).
- [14] A.L. Fetter and J.D. Walecka, *Quantum Theory of Many-Particle Systems*, McGraw-Hill, New York, 1971.
- [15] B. Jancovici, Nuovo Cimento 25, 428 (1962).
- [16] See e.g. J.M. Rax, *Physique des Plasmas*, Dunod, Paris 2005.
- [17] J. McOrist, D. B. Melrose, and J. I. Weise, J. Plasma Phys. 73, 495 (2007)
- [18] A. Bardasis and J.R. Schrieffer, Phys. Rev. **121**, 1050 (1961).

ρ_b [fm^{-3}]	Y_p [%]	Y_e [%]	Y_μ [%]	ω_{0e} [MeV]
0.16	3.70	3.63	0.07	6.15
0.32	8.57	5.95	2.62	10.25
0.48	13.03	7.98	5.05	13.48

TABLE I: Particle fractions for the baryonic densities under study. The electron plasmon frequency for $\rho_e = \rho_p$, used as a unit for the plots, is also given.

Figure captions.

Fig. 1 - The proton fraction (thick lines) and muon fraction (thin lines) as a function of total baryon density in neutron star matter. Microscopic calculations (taken as a reference) are compared with results from modern Skyrme forces.

Fig. 2 - The proton excitation spectra in the jelly model. The energy ω_{0e} is the electron plasmon energy at zero momentum, for $\rho_e = \rho_p$. The full line is obtained in the RPA scheme, the long-dashed line corresponds to the Vlasov approximation. The dashed-dotted line shows the effect of electron screening on the (RPA) proton spectrum.

Fig. 3 - Dispersion relation in the $pe\mu$ system (full lines), compared with the pe system (dashed lines), for three baryonic densities. The corresponding particle fractions are given in Tab. I. The dotted lines correspond to $\omega_i = v_{Fi}q$. The energy ω_{0e} is the electron plasmon energy for $\rho_e = \rho_p$.

Fig. 4 - Diagonal elements of the spectral-function matrix ($pe\mu$ system), for three momenta and $\rho_b = 0.32 \text{ fm}^{-3}$. The vertical lines indicate the energy at which the real part of the determinant of Eq. 7 vanishes. For the plasmon the dashed and full lines coincide. The energy ω_{0e} is the electron plasmon energy for $\rho_e = \rho_p$.

Fig. 5 - Diagonal elements of the spectral-function matrix ($pe\mu$ system), for three different densities and $q = 10 \text{ MeV}$. The energy ω_{0e} is the electron plasmon energy for $\rho_e = \rho_p$. The vertical lines indicate the energy at which the real part of the determinant of Eq. 7 vanishes. For the plasmon the dashed and full lines coincide.

Left: $pe\mu$ system; right: pe system.

Fig. 6 - Direction of the eigenvector associated with the plasmon mode.

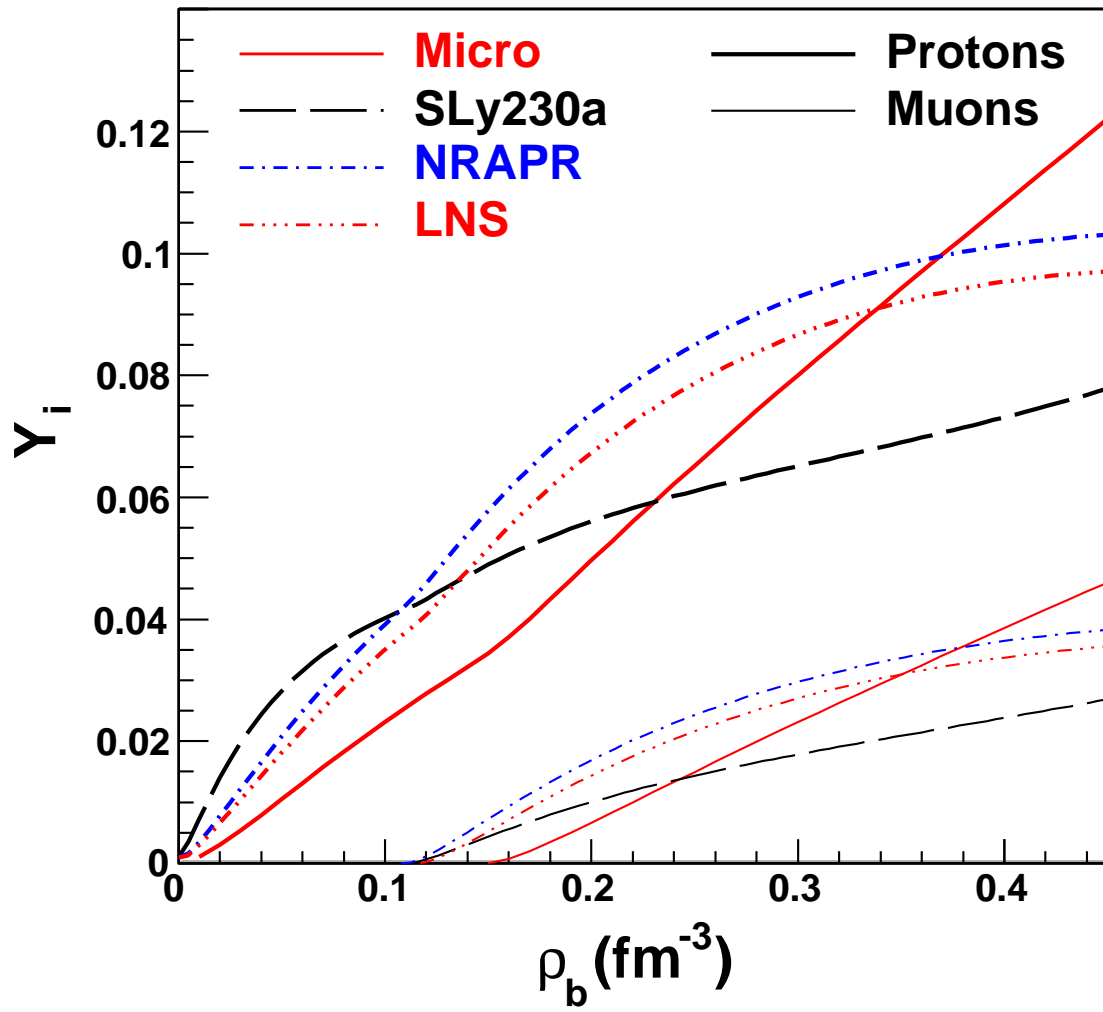


FIG. 1:

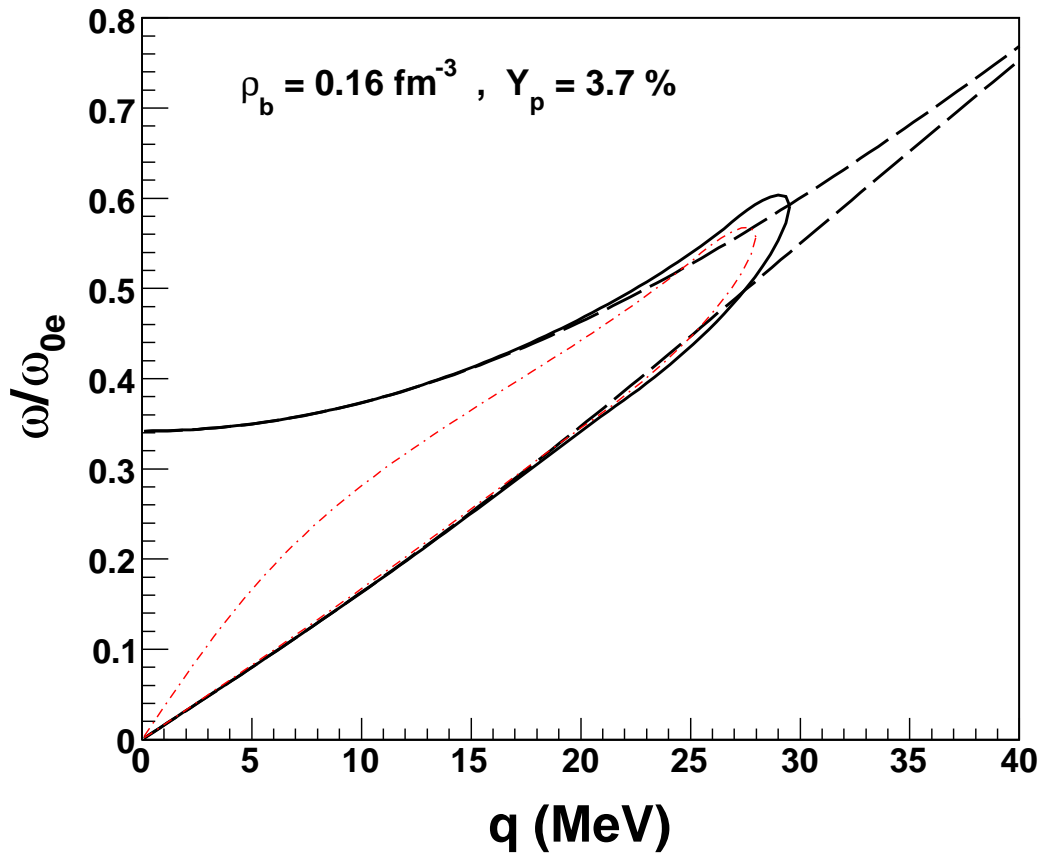


FIG. 2:

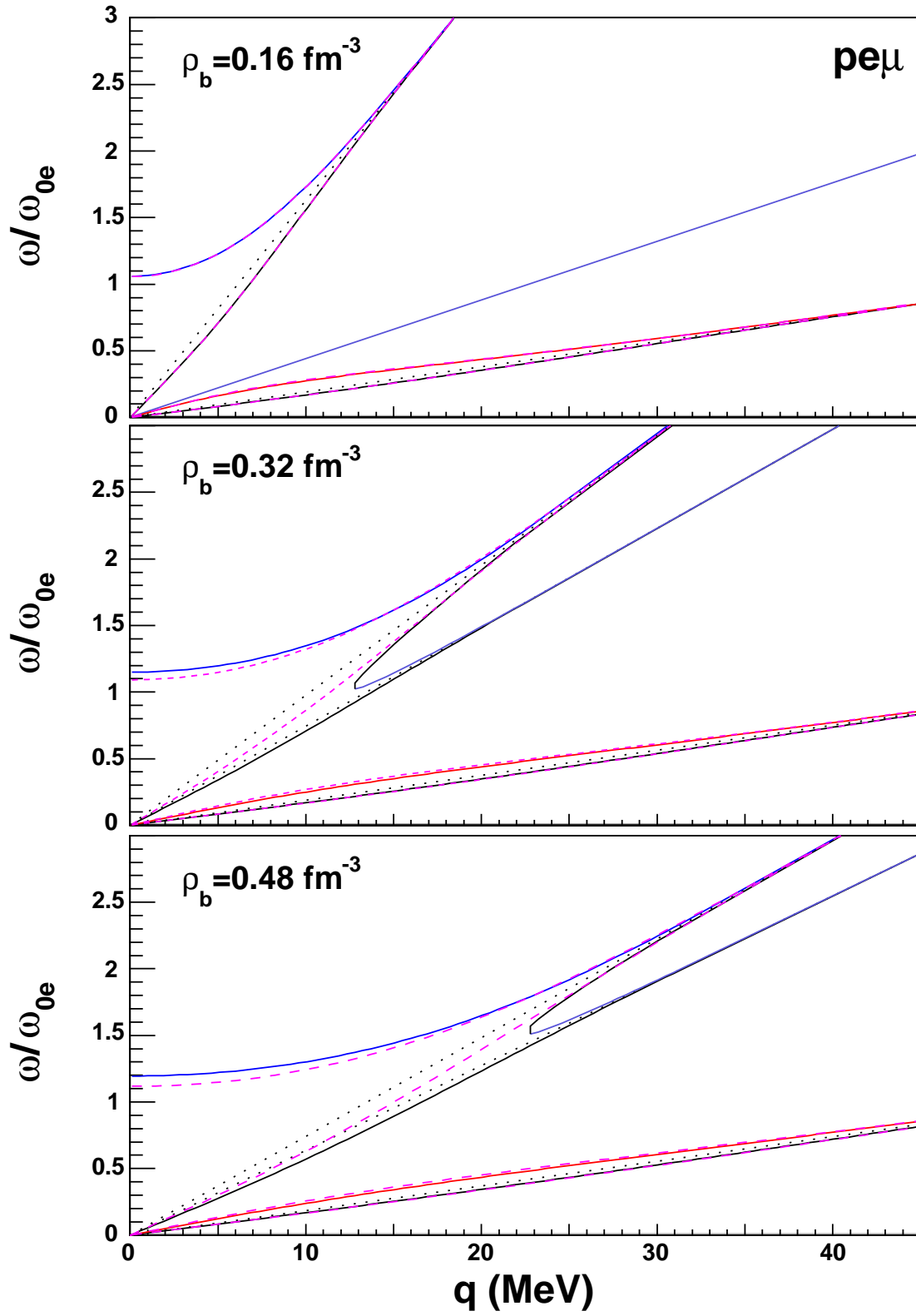


FIG. 3:

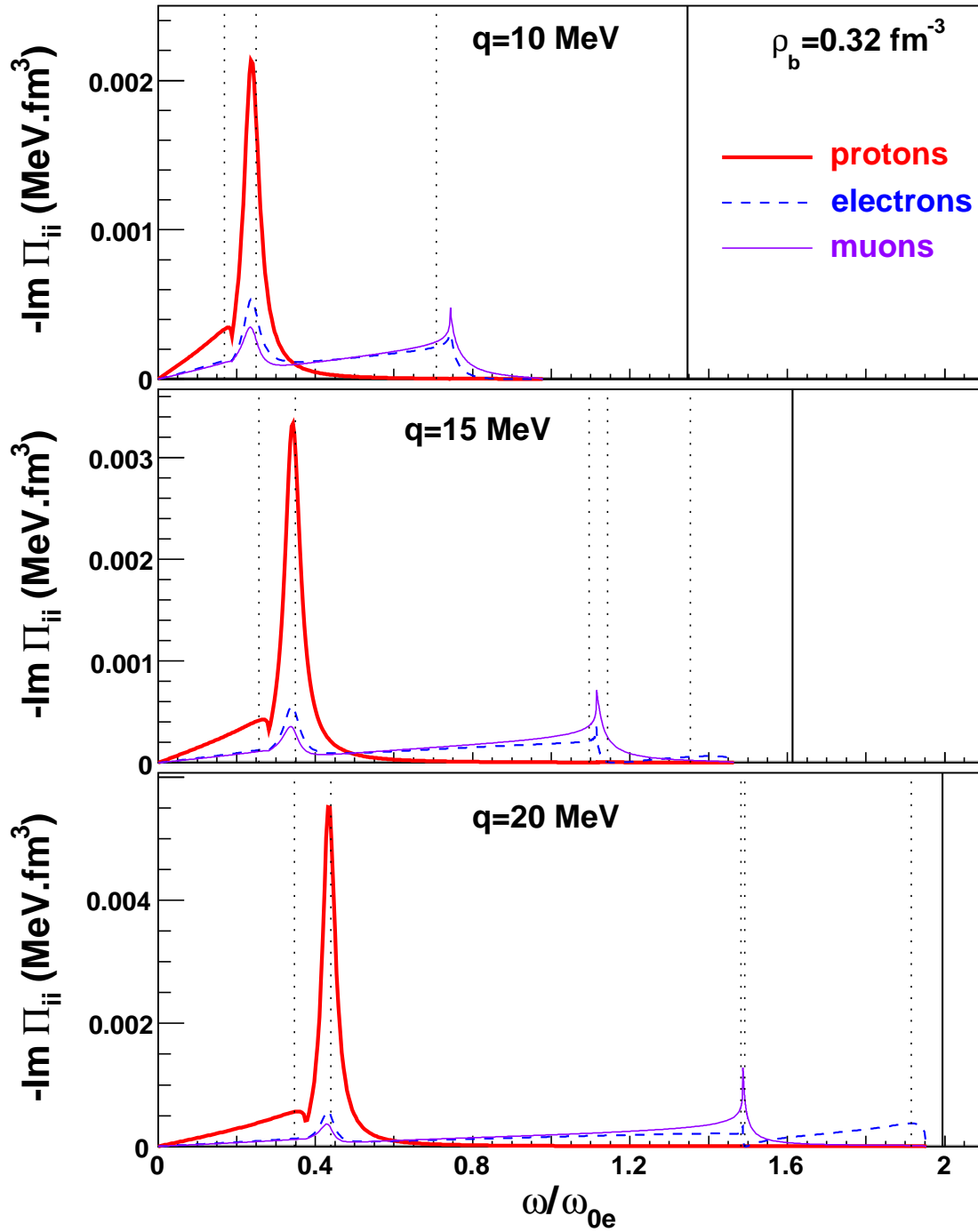


FIG. 4:

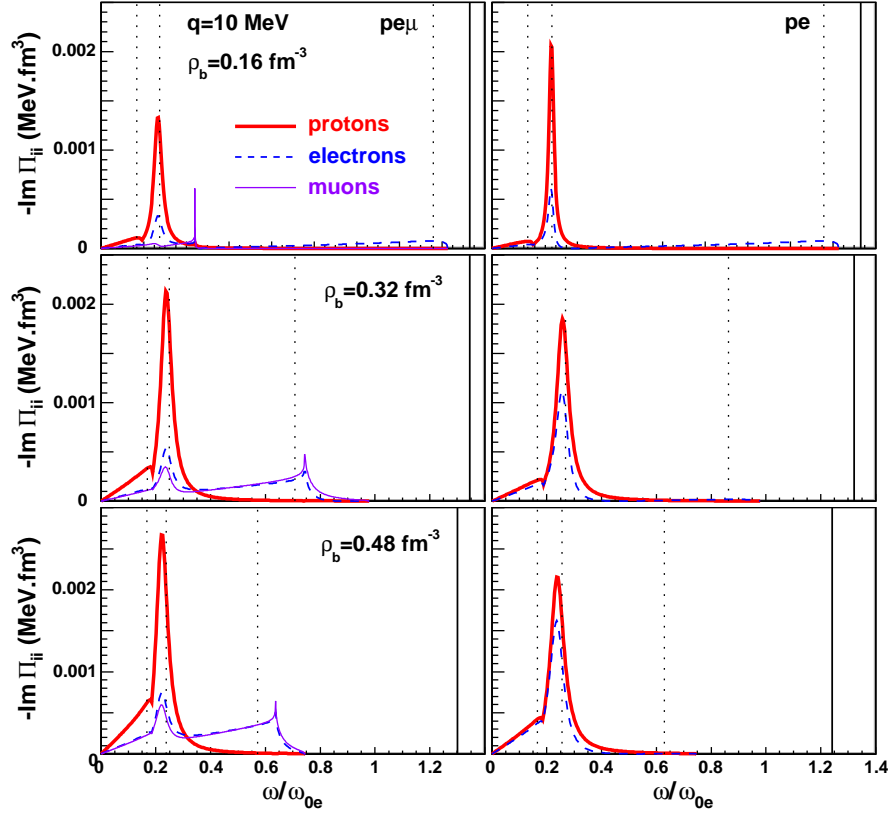


FIG. 5:

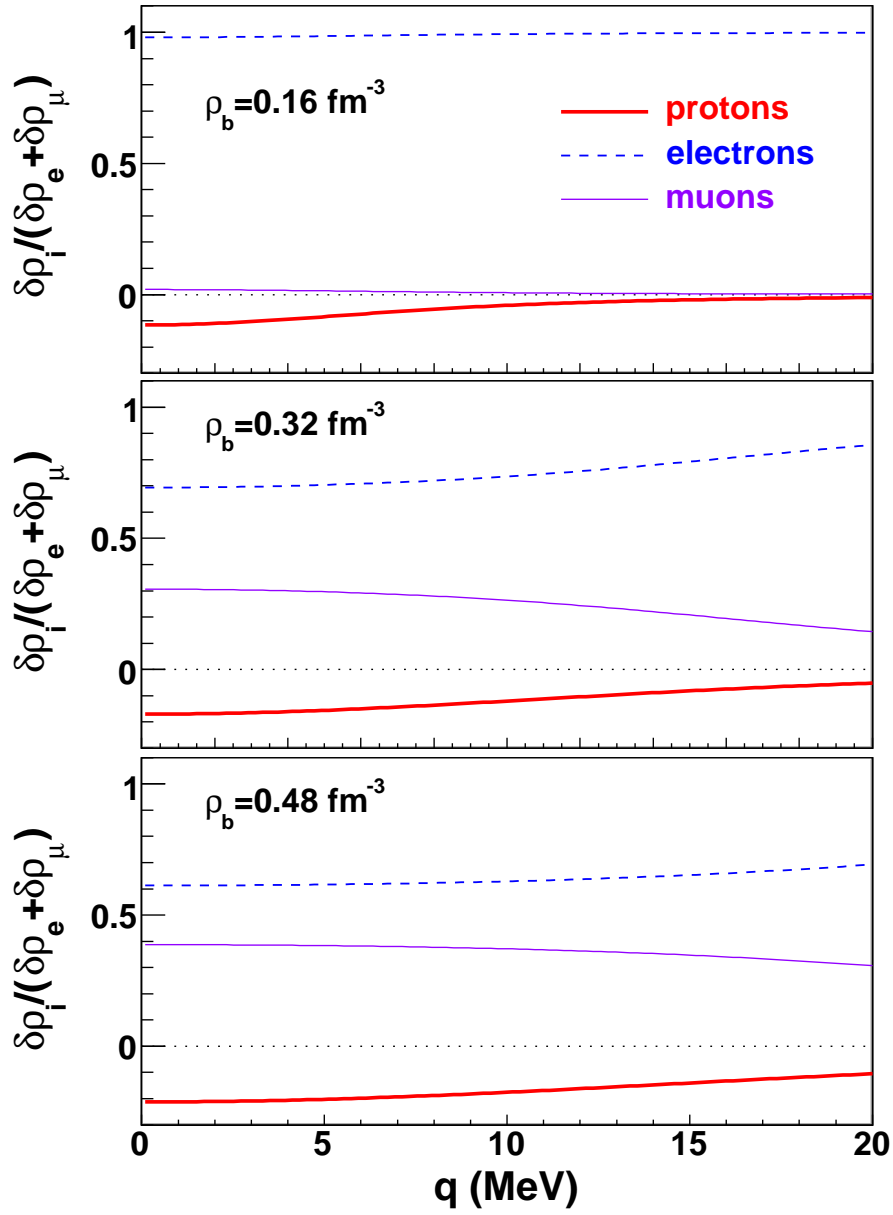


FIG. 6: